Nuclear Instruments and Methods in Physics Research, in press

Damage formation and optical absorption in neutron irradiated SiC

E. Wendler[(a)], Th. Bierschenk[(a)], F. Felgenträger[(a)], J. Sommerfeld[(a)], W. Wesch[(a)], D. Alber[(b)], G. Bukalis[(b)], L.C. Prinsloo[(c)], N. van der Berg[(c)], E. Friedland[(c)], J.B. Malherbe[(c)]

[(a)] Institut für Festkörperphysik, Friedrich-Schiller-Universität Jena, Max-Wien-Platz 1, 07743 Jena, Germany

[(b)] Campus Lise-Meitner, Abteilung F-A1, Elementanalytik, Helmholtz-Zentrum Berlin für Materialien und Energie GmbH, Hahn-Meitner-Platz 1, 14109 Berlin, Germany

[(c)] Department of Physics, University of Pretoria, 0002 Pretoria, South Africa

Abstract

The defect formation in neutron irradiated SiC was investigated by means of Rutherford backscattering spectrometry in channelling mode (RBS), optical absorption and Raman spectroscopy. The relative defect concentration determined by RBS increases linearly with the neutron fluence without any saturation in the investigated fluence region. The spectral dependence of the absorption coefficient α at photon energies below 3.2 eV is independent of the neutron fluence and corresponds to that observed in low-fluence ion implanted SiC. An increase of the defect concentration exhibits only in an increase of the absolute value of α. For photon energies above 3.3 eV again an exponential increase of the absorption coefficient is found but with a slope increasing with rising defect concentration. This absorption is assumed to be of the Urbach type. Around 1.56 eV a broad absorption band is observed which is most probably caused by divacancies $V_{Si}V_C$. The defects produced by the neutron irradiation of SiC result in a decrease of the peak intensity and a shift of the position of TO and LO Raman peaks towards lower wave numbers. The latter can be explained by tensile stress due to defects and mass increase of lattice atoms due to neutron capturing.

Keywords:

Silicon carbide, neutron irradiation, optical spectroscopy, Raman spectroscopy

1. Introduction

Radiation damage by energetic ions or neutrons in crystals disturbs the periodic arrangements of atoms and thus is connected with significant changes of the optical properties of the corresponding material. Although these effects can be observed also in the infrared reflectance (see e.g. [1, 2]), it is especially significant at photon energies below the fundamental absorption edge because the sharp edges of valence and conduction band are directly related to the perfect periodic lattice structure. Consequently, the optical absorption at photon energies within the region of transparency of the perfect crystal, i.e. below the fundamental absorption edge, is a sensitive tool to detect radiation damage. This was demonstrated for several materials as for instance SiC (see e.g. [3-6]), Si (see e.g. [7, 8]) and III-V compound semiconductors (see e.g. [9-11]). Point defect complexes and amorphous structures often exhibit a different spectral dependence of the absorption coefficient and a different refractive index change, which may allow separation of the contributions of the two structures within the implanted layers [4, 12]. Here we are only interested in the absorption coefficient being connected with point defects. It was found for B ion implanted SiC that the spectral dependence of the absorption coefficient seems not to change and increasing defect concentration results only in an increase of its absolute value [3]. Contrary to SiC, in GaAs both the spectral dependence and the absolute value of the absorption coefficient vary with the defect concentration introduced by ion [10] or neutron irradiation [13]. In the case of low defect concentrations and correspondingly low absorption coefficients, the study of ion implanted layers is limited due to their small layer thicknesses. The problem can be overcome by neutron irradiation which causes damage in the whole sample. In this contribution the optical subgap absorption as well as Raman spectra of SiC after neutron irradiation were investigated. For high neutron fluences the relative concentration of defects was measured with Rutherford backscattering spectroscopy (RBS) in channeling configuration.

2. Experimental Methods

Neutron irradiation of 4H-SiC and 6H-SiC was performed at the reactor BER II at the Helmholtz-Zentrum Berlin. Two different positions within the reactor were used namely (1) close to the core labelled DBVK and (2) in the reflector labelled DBVR. The neutron fluxes were for (1) 1.5×10^{14} $cm^{-2}s^{-1}$ (thermal neutrons), 6.8×10^{12} $cm^{-2}s^{-1}$ (epithermal neutrons), and 5.1×10^{13} $cm^{-2}s^{-1}$ (fast neutrons) and for (2) $6.0(5.4)\times10^{12}$ $cm^{-2}s^{-1}$ (thermal neutrons), $5.2(6.3)\times10^{9}$ $cm^{-2}s^{-1}$ (epithermal neutrons), and $1.1(1.2)\times10^{10}$ $cm^{-2}s^{-1}$ (fast neutrons). The numbers in parenthesis refer to one irradiation at a slightly different position. The times of exposure varied between 1.3 and 297.7 h. To convert the times into neutron fluences N_n only the epithermal and fast neutrons were taken into account. The temperature during irradiation was less than 50 °C.

The relative defect concentration n_{da} versus depth z was measured with RBS in channeling configuration at room temperature using 1.4 MeV He ions and a backscattering angle of 170°. The relative number of randomly displaced lattice atoms, n_{da}, was calculated with the computer code DICADA [14].

The optical absorption coefficient α was calculated from the transmission spectra measured using an UV-VIS spectrometer Cary 5000 operating in the range of spectroscopic wave numbers ν between 3000 and 30000 cm^{-1} corresponding to photon energies E between 0.37 and 3.7 eV (in the following text both units will be used). It is assumed that the samples are homogeneously damaged over the whole thickness, which allows a direct calculation of α basing on the Beer-Lambert law. In all cases the refractive index was assumed to be unchanged and the data for crystalline SiC were taken from Ref. 15.

Raman micro-spectroscopy was performed with a T64000 micro-Raman spectrometer from HORIBA Scientific, Jobin Yvon Technology. The Raman spectra were excited with the 514.5 nm line of an Inova 70v argon laser from Coherent and the 100x objective of an

Olympus microscope was used to focus the laser beam (spot size ~ 2µm) on the samples and also collected the backscattering Raman signal. An integrated triple spectrometer was used in the double subtractive mode to reject Rayleigh scattering and dispersed the light onto a liquid nitrogen cooled Symphony CCD detector. The spectrometer was calibrated with the silicon phonon mode at 520 cm^{-1}.

In our studies 6H-SiC samples were analysed with RBS/channeling and Raman spectroscopy and 4H-SiC samples with optical transmission and Raman spectroscopy. Only the latter samples were polished on both sides. These samples received such low fluences that the defect concentrations were, except for the highest fluence, too low to be detected with RBS/channeling. Consequently no RBS/channeling were performed on the 4H-SiC samples.

3. Results and discussion

Figure 1 shows the relative defect concentration measured over the first 0.4 µm of neutron irradiated 6H-SiC samples. The concentration is almost constant with the tendency to slightly decrease towards the surface. The same effect was observed for B ion implanted SiC for which an energy-fluence regime was calculated to achieve a thick homogeneously damaged layer, but the measured distributions also tend to decrease towards the surface [3]. The origin for that is not clear, but might be connected with the surface acting as sink and place for recombination of defects. To analyse the fluence dependence a mean value of the relative defect concentration was taken within the depth range of 0.025 to 0.4 µm, which is plotted in Fig. 2. A linear increase of the mean value n_{da} with rising neutron fluence N_n is found which can be represented by $n_{da} = N_n \cdot 2.6\times10^{-21}$ cm^2. It was found previously that also the carrier concentration and their mobility decrease linearly in heavily doped SiC with rising neutron fluence [16]. Point defects are known to trap free carriers and act as scattering centres and thus may reduce the carrier mobility. Consequently, in agreement with the RBS data shown here also the results from electrical measurements point to a linear increase of the number of

defects produced with increasing neutron fluence [16]. It is to be expected that this holds well also for neutron fluences lower than those for which RBS analysis is possible. Therefore, the relation between relative defect concentration and neutron fluence given above is used to convert the fluences into defect concentrations which is useful for comparison with data obtained for ion implanted SiC (see below).

In Fig. 3 the spectral dependence of the absorption coefficient is shown for the neutron irradiated 4H-SiC samples. The appearance is strikingly similar to that found for low-fluence B implanted 6H-SiC [3]. A similar behaviour is also observed in SiC irradiated with Au and Xe ions at 400 °C [5]. The absorption coefficient versus wave number is characterized by a background increasing exponentially with increasing wave number and by a broad absorption band. When normalizing the data in Fig. 3 to that of the lowest neutron fluence (not shown), they all show the same spectral dependence for wave numbers below about 25800 cm^{-1} (corresponding to 3.2 eV). This corresponds well to the results for B ion implanted SiC mentioned above [3].

The absorption band around wave numbers of 12580 cm^{-1} (corresponding 1.56 eV) was previously reported for neutron irradiated SiC [17]. In that paper the relation to a defect involving a Si vacancy was concluded by comparison of the annealing characteristics of the absorption band with that of an electron-spin-resonance line, which can be attributed to single Si vacancies. The existence of divacancies in ion irradiated SiC was deduced with the help of positron spectroscopy [18, 19]. With this method divacancies were also found to be a dominating defect in neutron irradiated SiC [20]. This result follows both from the analysis of the *S* parameter and from positron life-time spectroscopy [18-20]. In irradiated silicon the divacancy is also a common defect and it is connected with a pronounced absorption band being observed at photon energies below the fundamental absorption edge [21]. Therefore it seems to be reasonable to assume that the absorption band in SiC is caused by the divacancy $V_{Si}V_C$. The data presented in Fig. 3 indicate a second weak absorption band around 9300 cm^{-1}

(corresponding to 1.15 eV) for the four lowest neutron fluences applied. It might be possible that this weak band also belongs to the divacancy. This suspicion is inspired from the similarity to silicon for which the divacancy is connected with two further less strong absorption bands [21].

In the spectral range $16000\ \mathrm{cm^{-1}} < \nu < 25800\ \mathrm{cm^{-1}}$ ($2\ \mathrm{eV} < E < 3.2\ \mathrm{eV}$) the absorption coefficient follows the dependence $\alpha \propto \exp(E/E_{01})$ with $E_{01} = 0.7\ \mathrm{eV}$ independent of the neutron fluence. The same constant value was found for Au and Xe ions implanted into 4H- and 6H-SiC at 400 °C [5] – a temperature for which no amorphisation is to be expected because it is above the critical value [22]. It is worth mentioning that no differences are found between 6H- and 4H-SiC. The similarity of damage formation in both SiC polytypes was also concluded from annealing experiments performed on neutron irradiated SiC [17].

From Fig. 3 it can be seen that close to the direct band edge of 4H-SiC for $\nu > 26600\ \mathrm{cm^{-1}}$ ($E > 3.3\ \mathrm{eV}$) again an exponential increase of the absorption coefficient α according to $\alpha \propto \exp(E/E_{02})$ is found. This spectral range (which was not resolved in Ref. 3) is shown more clearly in Fig. 4 which plots the absorption coefficient versus the photon energy E. In this photon energy range the slope represented by E_{02} increases with increasing neutron fluence (corresponding to an increasing defect concentration) from $E_{02} = 0.095\ \mathrm{eV}$ for the lowest neutron fluence plotted in Fig. 4, to $E_{02} = 0.23\ \mathrm{eV}$ for the highest. The occurrence of two different exponential ranges of the absorption coefficient versus the photon energy was also found in ion implanted GaP [10]. In this material the parameter E_{02} exhibits a pronounced [10] and E_{01} a very weak dependence on the defect concentration [10, 23]. Also in the case of ion irradiated silicon the divacancy absorption band already mentioned above is superimposed by an exponentially increasing background absorption the slope of which varies only slightly with the defect concentration; the spectral range close to the direct band gap was not resolved [8]. From these findings it is supposed that the exponential absorption with the parameter E_{01}

being not or only slightly dependent on the defect concentration is connected with the indirect band gap in these materials. In the direct materials GaAs and InP only one exponential increase of the absorption coefficient with photon energy is found with the parameter E_{02} being clearly dependent on the defect concentration [10, 11].

Exponential subgap absorption tails in crystalline materials are usually called Urbach tails [24]. They are observed in highly doped semiconductors and at elevated temperatures [25, 26]. In the former case the tailing energies are of the order of few tenth of an eV and they show a dependence on doping concentration. In the latter the tailing energies increase with rising temperature. It was shown for Si by molecular dynamics calculations and RBS channeling measurements that each divacancy is surrounded by 18 atoms which are displaced more than 0.02 nm from their ideal lattice position [27]. Thus, a simple picture of a defective crystal could be that it contains point defects like vacancies, divacancies and interstitial atoms each of them being surrounded by a halo of slightly displaced lattice atoms. This could be regarded as a snap-shot of a perfect crystal at an elevated temperature, which also should be characterized by a large number of slightly displaced lattice atoms. In this respect the mentioned absorption tails may have a similar physical origin. We assume that these suspicions hold well only for the tails close to the direct band gap with the parameter E_{02}. The broad background tails in case of SiC, GaP and Si with tailing energy E_{01} may have a different physical origin.

Figure 5 summarises the measured absorption coefficients α versus the neutron fluence N_n applied for two different wave numbers. Additionally, the absorption coefficient in the maximum of the absorption band is shown after subtracting the background absorption. To compare the results with those obtained for B ion irradiated SiC α is plotted versus the relative defect concentration n_{da} into which the neutron fluences are converted as explained above. For both conditions a uniform almost linear dependence α (n_{da}) is found. This clearly

confirms that the optical absorption is related to the defects produced by the irradiation with energetic particles. It also means that there is some correlation between the absorption within the band and the background absorption, which could be taken as an indication that both have the same origin. The four data points at very low concentrations belong to neutron irradiations which were performed at position (2) with a significantly higher rate of thermal neutrons in relation to that of fast neutrons (see chapter 2). Thermal neutrons were not taken into account when converting the exposure times to neutron fluences (see chapter 2). Therefore, the systematic deviation of the data for the four lowest neutron fluences from the straight linear dependence in Fig. 5 suggests that the influence of the thermal neutrons cannot be completely neglected. From Fig. 5 it can be seen that the data for the B ion implanted samples with the highest defect concentrations tend to deviate from the linear slope. This suggests that more complex defect structures start to form for relative defect concentrations at $n_{da} > 0.1$.

The Raman spectra measured on neutron irradiated 6H-SiC are presented in Fig. 6a. For comparison purposes Fig. 6b plots the spectrum of a virgin 6H-SiC sample and a spectrum measured on a SiC sample fully amorphised by Ag ion irradiation. The figure shows that the main TO and LO Raman peaks decrease in height and shift to lower wave numbers with increasing neutron fluences. A decrease in peak intensity is typical for increasing defect concentration [28], however the bathochromic shift of the peaks is not typical and is usually an indication of tensile stress experienced by a particular bond between atoms. As there is no external force that could be responsible for stress in this instance the observed effects are caused changes in the SiC structure due the neutron irradiation. Besides the stress due to lattice defects it is suggested that during the radiation process neutrons are absorbed by both C and Si atoms to form the stable isotopes ^{13}C, ^{14}C, ^{29}Si and ^{30}Si. An increase in mass would lengthen the bonds between the atoms and cause a bathochromic shift as the vibrational energy of a chemical bond is influenced by the masses of the atoms involved, for example the 520.7 cm^{-1} silicon Raman band occurs at 512.3 and 503.9 cm^{-1} for the isotopes ^{29}Si and ^{30}Si

respectively [29]. This result is in line with an increase of the size of the crystal lattice as previously reported for neutron irradiated SiC [30]. For the highest neutron fluence applied these peaks degenerate to broad plateau-like structures. However, this spectrum does not correspond to the spectrum obtained for the Ag ion implanted SiC layer being fully amorphised (see Fig. 6b). This is in agreement with the result from the RBS analysis which yields a relative defect concentration of about 0.2 for the neutron irradiated sample (see Fig. 1). As a summery the LO peak position and the normalised LO peak intensity are given in Fig. 7. Similar results are also found for the TO Raman lines (not shown). Surprisingly these two quantities do not exhibit a linear dependence on neutron fluence or defect concentration, respectively, as was shown above for the optical subgap absorption and found for the electrical properties [16]. Obviously the Raman signal has a completely different susceptibility to neutron-induced defects in SiC. A significant decrease of the Raman intensity occurs for neutron fluences between 5×10^{17} and 1×10^{19} cm^{-2}. For these fluences the absorption coefficient cannot be measured anymore in that way because the samples become opaque. Further investigations are necessary to understand the discrepancy in the fluence dependences.

4. Summary

The defect evolution in neutron irradiated SiC was studied using Rutherford Backscattering Spectrometry (RBS), optical absorption as well as Raman spectroscopy. Particularly the investigation of the optical absorption below the fundamental absorption edge is a sensitive tool to detect radiation damage.

The relative defect concentration determined by RBS for a given neutron fluence is almost constant in the depth region investigated with a tendency to slightly decrease towards the surface. The linear increase of the relative defect concentration with the neutron fluence is in agreement with previously published results of electrical measurements.

Below the fundamental absorption edge the spectral dependence of the absorption coefficient of the neutron irradiated samples is characterized by absorption tails exponentially depending on photon energy and by a broad absorption band. In the photon energy range $2\ eV < E < 3.2\ eV$ the spectral dependence is equal for all neutron fluences which is similar to the behaviour observed in low-fluence boron implanted 6H-SiC. An absorption band around 1.59 eV is attributed to the existence of divacancies $V_{Si}V_C$. Close to the direct band edge ($3.3\ eV < E < 3.5\ eV$) a different slope of the absorption coefficient with photon energy is found, which increases with increasing defect concentration. This absorption is assumed to be of the Urbach type. The occurrence of two ranges with a different increase of the absorption coefficient with photon energy seems to be representative for indirect semiconductors.

The linear dependence of the absorption coefficient on the relative defect concentration found for both neutron irradiation and low-fluence boron implantation confirms that the optical absorption is related to the defects produced by the irradiation with energetic particles.

A decrease of the intensities of the main TO and LO Raman peaks and a shift to lower wave numbers with increasing neutron fluence are found which are typical for an increasing defect concentration. The shift can be explained by tensile strain caused by defects and the mass increase of lattice atoms due to neutron capturing. However, the reason for the discrepancies in the fluence dependences of the absorption coefficient and peak position and intensity of the Raman lines is not yet clear and needs further investigation.

5. Acknowledgements

The financial support of the Bundesministerium für Bildung und Forschung in Germany within the International Cooperation in Research and Education under Project-No. SUA 08/028 and the National Research Council of South Africa under Project No. UID 69445 is gratefully acknowledged.

References

[1] D.J. Brink, J.B. Malherbe, J. Camassel, Nucl. Instr. and Methods B 267 (2009) 2716.

[2] H.H. Zhang, C.H. Zhang, B.S. Li, L.H. Han, Y. Zhang, Nucl. Instr. and Methods B 268 (2010) 2318.

[3] E. Wendler, A. Heft, U. Zammit, E. Glaser, M. Marinelli, W. Wesch, Nucl. Instr. and Methods B 116 (1996) 298.

[4] E. Wendler, G. Peiter, J. Appl. Phys. 87 (2000) 7679.

[5] S. Sorieul, J.-M. Costantini, L. Gosmain, G. Calas, L. Thomé, J. Phys. Condens. Materr 18 (2006) 8493.

[6] M.Musomeci, L. Calcagno, M.G. Grimaldi, G. Foti, Appl. Phys. Lett. 69 (1996) 468.

[7] W. Wesch, E. Glaser, G. Götz, H. Karge, R. Prager, phys. stat. sol. (a) 65 (1981) 225.

[8] E. Wendler, K. Gärtner, W. Wesch, U. Zammit, K.N. Madhusoodanan, Nucl. Instr. and Methods B 85 (1994) 528.

[9] W. Wesch; E. Wendler, G. Götz, N.P. Kekelidse, J. Appl. Phys. 65 (1989) 519.

[10] E. Wendler, W. Wesch, G. Götz, phys. stat. sol. (a) 112 (1989) 289.

[11] E. Wendler, T. Opfermann, P.I. Gaiduk, J. Appl. Phys. 82 (1997) 5965.

[12] W. Wesch, E. Wendler, G. Götz, Nucl. Instrum. and Methods B 22 (1987) 532.

[13] R. Coates, E.W.J. Mitchell, Proc. of the Intern. Conf. on Defects in Semiconductors, Reading 1972, 95.

[14] K. Gärtner, Nucl. Instrum and Methods B 227 (2005) 522.

[15] Data are taken from http://refractiveindex.info/?group=CRYSTALS&material=SiC, July 2011.

[16] E. Almaz, St. Stone, Th. E. Blue, J.P. Heremans, Nucl. Instrum. and Methods A 622 (2010) 200.

[17] M. Okada, K. Atobe, M. Nakagawa, S. Kannazawa, I. Kanno, I. Kimura, Nucl. Instrum. and Methods B 166-167 (2000) 399.

[18] G. Brauer, W. Anwand, P.G. Coleman, A.P. Knights, F. Plazaola, Y. Pacaud, W. Skorupa, J. Störmer, P. Willutzki, Phys. Rev. B 54 (1996) 3084.

[19] C.Y. Zhu, C.C. Ling, G. Brauer, W. Anwand, W. Skorupa, J. Phys, D Appl. Phys. 41 (2008) 195304.

[20] Y. Liu, G. Wang, S. Wang, J. Yang, L. Chen, X. Qin, B. Song, B. Wang, X. Chen, Phys. Rev. Lett. 106 (2011) 087205.

[21] L.J. Cheng, J.C. Corelli, J.W. Corbett, G.D. Watkins, Phys. Rev. 152 (1966) 761.

[22] W.J. Weber, L. Wang, Y. Zhang, W. Jiang, I.-T. Bae, Nucl. Instrum. and Methods B 266 (2008) 2793.

[23] W. Wesch, E. Wendler, J. Kaczanowski, A. Turos, Nucl. Instrum. and Methods B 85 (1994) 533.

[24] N.F. Mott, E.A. Davies, Electronic Processes in Non-crystalline Materials 2nd edn, Oxford: Clarendon 1979.

[25] V.L. Bonch-Bruevich, phys. stat. sol. 42 (1970) 35; K. Unger, in: Optoelektronik in $A_{III}B_{V}$-Halbleitern, Sonderdruck aus: Wissenschaftliche Zeitschrift der Karl-Marx-Universität Leipzig, Mathematisch-Naturwissenschaftliche Reihe, 20. Jahrgang (1971), Heft 1 and 2, p. 93.

[26] J. Szczyrbowski, phys. stat. sol. (b) 79 (1977) K 43.

[27] B. Weber, E. Wendler, K. Gärtner, D.M. Stock, W. Wesch, Nucl. Instrum. and Methods B 118 (1996) 113.

[28] S. Sorieul, J-M Costantini, L Gosmain, L. Thomé, J-J Grob, J. Phys. Condens. Matter, 18 (2006) 5235.

[29] V.G. Plotnichenko, V.O. Nazaryants, E.B. Kryukova, V.V. Koltashev, V.O. Sokolov, E.M. Dianov, A.V. Gusev, V.A. Gavva, T.V. Kotereva, M.F. Churbanov, Appl. Opt. 50(23) (2011) 4633.

[30] T. Yano, Y. Yamamoto, T. Iseki, J. Nucl. Mat. 307-311 (2002) 1102.

Figure captions:

Fig. 1

Relative defect concentration versus depth, $n_{da}(z)$, neutron irradiated SiC. The neutron fluences N_n are given in cm^{-2} taking into account only epithermal and fast neutrons.

Fig. 2

Mean relative defect concentration n_{da} of neutron irradiated SiC versus the neutron fluences N_n. The line represents a linear increase of n_{da} with N_n.

Fig. 3

Absorption coefficient α versus the spectroscopic wave number ν for neutron irradiated SiC. The neutron fluences N_n are given in cm^{-2}. For comparison the absorption coefficient of the SiC substrate is included.

Fig. 4

Absorption coefficient α versus the photon energy E for neutron irradiated SiC. The neutron fluences N_n are given in cm^{-2}. The exponential absorption tails close to the direct band edge are indicated by the straight lines.

Fig. 5

Absorption coefficient α versus the relative defect concentration n_{da} for neutron and B^+ irradiated SiC. For comparison the upper abscissa gives the neutron fluences N_n. α is plotted for wave numbers $\nu = 5000\ cm^{-1}$ and $16000\ cm^{-1}$ corresponding to photon energies $E = 0.62$ eV and 1.98 eV, respectively. Additionally the absorption in the maximum of the

absorption band is shown after subtracting the background absorption. The lines indicate linear dependencies.

Fig. 6

Raman intensity versus the Raman shift (a) for neutron irradiated 6H-SiC and (b) for the corresponding unirradiated 6H-SiC. In part (b) the spectrum of SiC after complete amorphisation by Ag ion implantation is shown for comparison.

Fig. 7

LO peak position and normalised LO peak intensity versus the neutron fluence N_n. Results are given for neutron irradiated 6H-SiC (see Fig. 6) and 4H-SiC (spectra not shown). For comparison the upper abscissa shows the corresponding relative defect concentration n_{da}.

Fig. 1

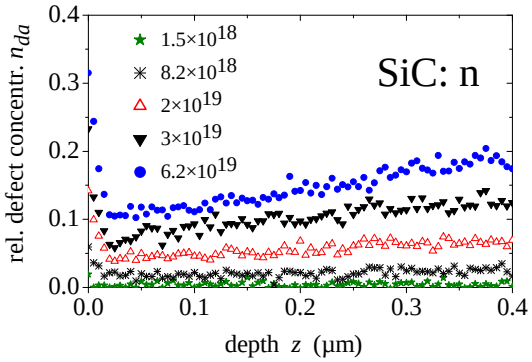
SiC: n
1.5×10^18
8.2×10^18
2×10^19
3×10^19
6.2×10^19
rel. defect concentr. n_{da}
depth z (μm)
0.0
0.1
0.2
0.3
0.4

Fig. 2

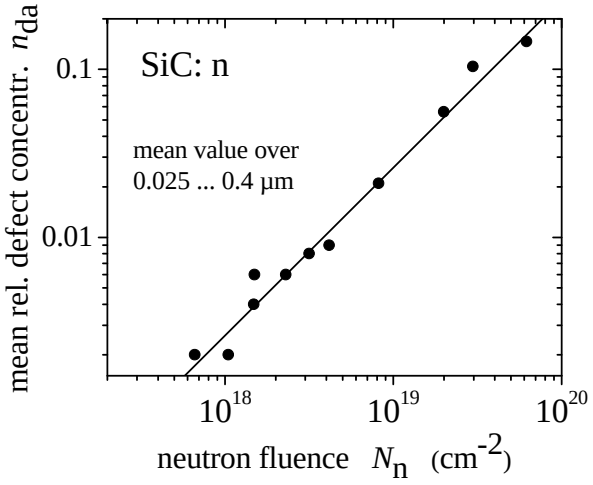
SiC: n
mean value over
0.025 ... 0.4 µm
mean rel. defect concentr. n_{da}
0.1
0.01
10^{18}
10^{19}
10^{20}
neutron fluence N_n (cm^{-2})

Fig. 3

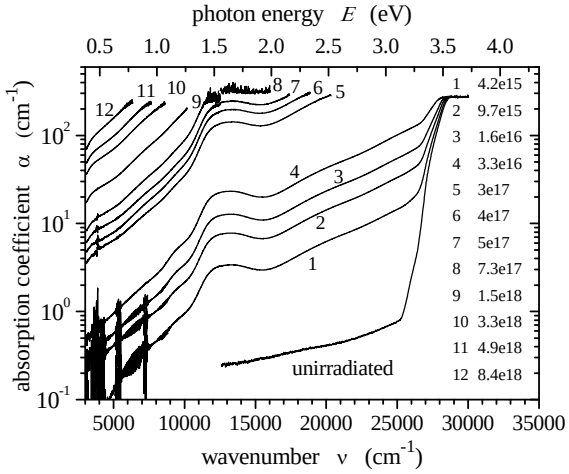
photon energy E (eV)
0.5 1.0 1.5 2.0 2.5 3.0 3.5 4.0
absorption coefficient α (cm-1)
10^2
10^1
10^0
10^-1
5000 10000 15000 20000 25000 30000 35000
wavenumber ν (cm-1)
1 4.2e15
2 9.7e15
3 1.6e16
4 3.3e16
5 3e17
6 4e17
7 5e17
8 7.3e17
9 1.5e18
10 3.3e18
11 4.9e18
12 8.4e18
unirradiated

Fig. 4

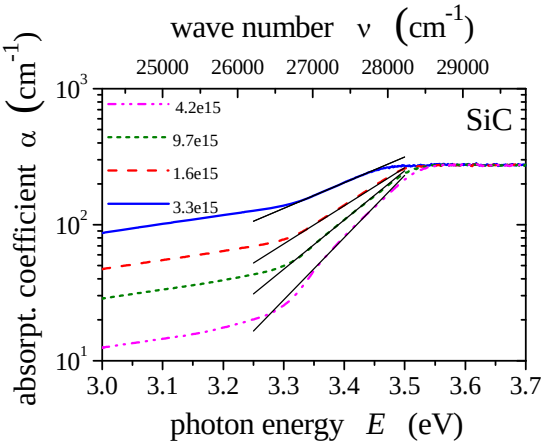
wave number ν (cm-1)
25000 26000 27000 28000 29000
absorpt. coefficient α (cm-1)
10^3
10^2
10^1
4.2e15
9.7e15
1.6e15
3.3e15
SiC
3.0 3.1 3.2 3.3 3.4 3.5 3.6 3.7
photon energy E (eV)

Fig. 5

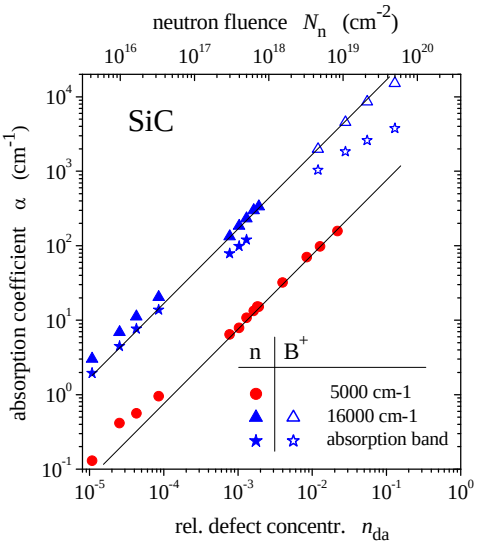
neutron fluence N_n (cm^{-2})
10^{16} 10^{17} 10^{18} 10^{19} 10^{20}
SiC
absorption coefficient α (cm^{-1})
10^{4} 10^{3} 10^{2} 10^{1} 10^{0} 10^{-1}
n | B^{+}
5000 cm-1
16000 cm-1
absorption band
10^{-5} 10^{-4} 10^{-3} 10^{-2} 10^{-1} 10^{0}
rel. defect concentr. n_{da}

Fig. 6

(a)

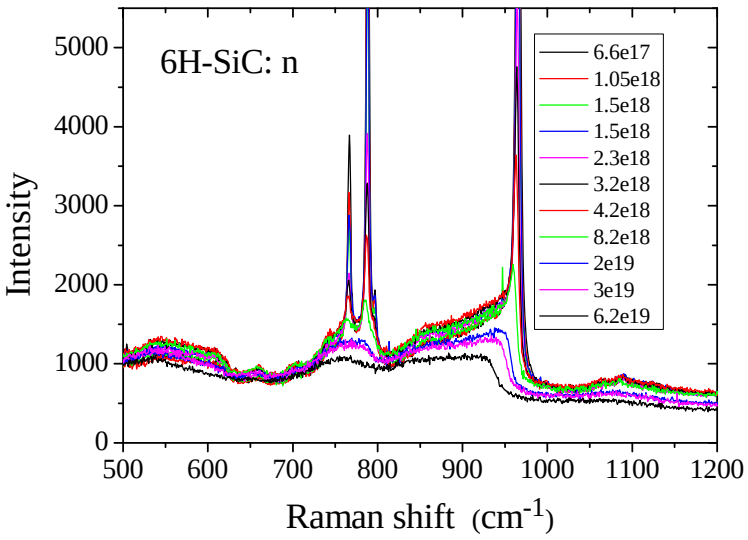
6H-SiC: n
6.6e17
1.05e18
1.5e18
1.5e18
2.3e18
3.2e18
4.2e18
8.2e18
2e19
3e19
6.2e19
Intensity
Raman shift (cm-1)
0
1000
2000
3000
4000
5000
500
600
700
800
900
1000
1100
1200

(b)

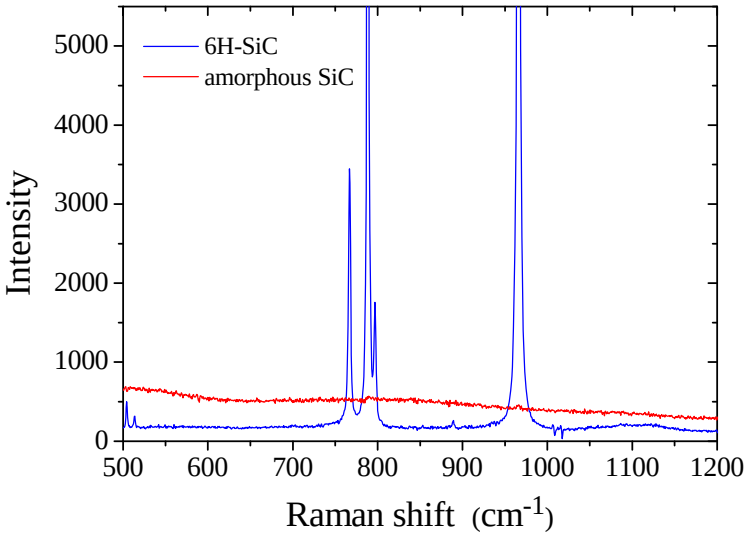
6H-SiC
amorphous SiC
Intensity
Raman shift (cm-1)
0
1000
2000
3000
4000
5000
500
600
700
800
900
1000
1100
1200

Fig. 7

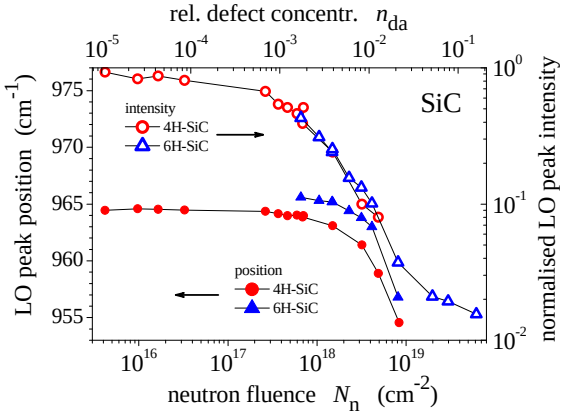
rel. defect concentr. n_{da}
10^{-5}
10^{-4}
10^{-3}
10^{-2}
10^{-1}
10^{0}
10^{-1}
10^{-2}
975
970
965
960
955
SiC
intensity
4H-SiC
6H-SiC
position
4H-SiC
6H-SiC
LO peak position (cm^{-1})
normalised LO peak intensity
10^{16}
10^{17}
10^{18}
10^{19}
neutron fluence N_n (cm^{-2})